

Different background conductances in the tunneling characteristics of $\text{Bi}_2\text{Sr}_2\text{CaCu}_2\text{O}_8$ -based junctions

A. M. Cucolo, R. Di Leo, A. Nigro, P. Romano, and M. Carotenuto

Dipartimento di Fisica, Università di Salerno, I-84081 Baronissi, Italy

(Received 28 May 1993)

Gaplike structures superimposed on different background behaviors are observed in the tunneling characteristics of Bi-Sr-Ca-Cu-O-based planar junctions. In the case of constant background, the conductance curves are quantitatively modeled by assuming a modified BCS density of states for the high- T_c material from which $\Delta = 20 \pm 2$ meV is inferred. In the case of linear backgrounds, we have studied the influence that increasing slopes have on the Bi-Sr-Ca-Cu-O superconducting structures. For extremely anomalous backgrounds, we have analyzed the effect that a zero-bias conductance peak, depending on its voltage amplitude, has on the superconducting structures of both the high- T_c material and the conventional counterelectrode.

I. INTRODUCTION

Anomalous high-bias (background) conductances are often observed in the tunneling characteristics of high- T_c superconductors (HTS).¹ Increasing linear backgrounds²⁻⁵ or, in some cases, a decreasing conductance dependence with voltage^{6,7} have been reported. On the other hand, only few examples of constant and, for much higher energies, parabolic behavior, as in conventional junctions, can be found in the literature.⁸⁻¹⁰

It is well known that in a tunnel junction at low temperatures the conductance is proportional both to the tunnel probability $P(E)$ and to the electrode densities of states (DOS) $N(E)$. However, in a good quality conventional junction the range of variations of these quantities is quite different. The DOS study is indeed of interest in characterizing the superconducting state which is described in terms of $N_S(E)$ variations at low energies (few meV), for which $P(E)$ can be considered constant. The $P(E)$ analysis is instead carried out at higher biases (hundreds of meV), for which normal DOS N_N are involved that vary slowly for conventional metal electrodes.

Unfortunately, for HTS-based junctions it is difficult to separate the two contributions and anomalous conductances at high bias cannot be unambiguously related to barrier or to DOS effects. In particular, explanations in terms of $P(E)$ have been given in which inelastic tunneling processes are responsible for linear backgrounds.¹¹ Alternatively, anomalous normal DOS have been proposed. Anderson and Zou¹² have modeled the linear term from the spectrum of holon and spinon excitations in a bidimensional resonating-valence-bond state. Varma *et al.*¹³ have formulated the marginal Fermi-liquid theory in which strong correlation effects are developed near the metal-insulator transition. Phillips¹⁴ separates the DOS in two different terms responsible for the superconducting and normal properties.

In lack of a final answer, through a different approach to the problem, in this paper we analyze the different backgrounds of Bi-Sr-Ca-Cu-O based junctions and their influence on the tunneling characteristics of the high- T_c

material. We present data on the 2-2-1-2 Bi-Sr-Ca-Cu-O system, for which, in spite of the numerous tunneling studies, there is still a wide uncertainty about the value of the energy gap. Indeed $2\Delta(0)/k_B T_c$ values ranging from 3 to 14 have been reported.¹ Among the possible reasons responsible for the spreading of the experimental data, we have focused our attention on the conductance backgrounds that these junctions show and on the superconducting double structure that is not always well resolved in the tunneling spectra of the Bi-Sr-Ca-Cu-O system so adding even more arbitrariness in the determination of the "true" value of the energy gap.

II. EXPERIMENTS

Our analysis includes more than 100 tunneling characteristics. All the junctions were fabricated on liquid etched (1% Br in methanol, by volume) $\text{Bi}_2\text{Sr}_2\text{CaCu}_2\text{O}_8$ single crystals with resistive $T_c \geq 80$ K and $\Delta T_c \leq 3$ K. The use of a chemical etching bath has given reproducible conductance curves on YBaCuO single crystals⁴ and films¹⁵ and it has been demonstrated that it is also effective at removing nonsuperconducting species from Bi-Sr-Ca-Cu-O thin-film surfaces.¹⁶

After a short air exposition (≈ 30 min) of the etched crystals, cross-type junctions were completed by thermally evaporating thin-film counterelectrodes. Pb, Pb-Bi, and Au have been used to check the reproducibility of the data independently from the nature of the used counterelectrode. Differential resistances were measured by a standard low-frequency lock-in technique.

A. Constant backgrounds

Flat background conductances are often observed in the tunneling characteristics of Bi-Sr-Ca-Cu-O based junctions,^{8,17-19} but they are not routinely found among the cuprate superconductors. In this sense, they seem to be quite peculiar of the Bi-Sr-Ca-Cu-O system. We have found them in about 60% of the measured junctions.

In Fig. 1 the I - V characteristic and the normalized differential conductance vs voltage (full lines) of a Bi-Sr-

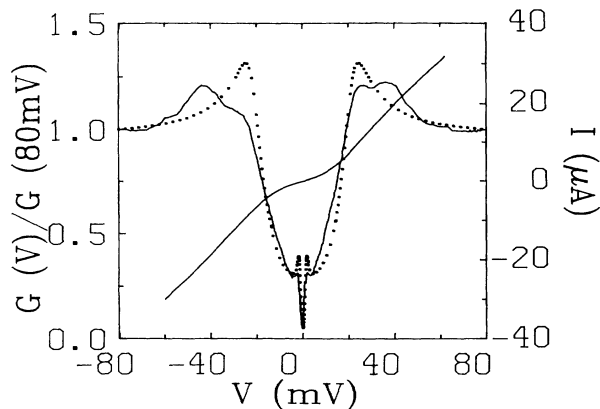


FIG. 1. I - V and normalized conductance characteristics of a Bi-Sr-Ca-Cu-O/Pb junction at $T=4.2$ K (full lines). The dotted line is the theoretical fitting obtained from expression (1) with $\Delta=20$ meV, $\Gamma=6$ meV. $\Delta_{pb}=1.3$ meV has been used.

Ca-Cu-O/Pb junction at $T=4.2$ K are shown. The main features observed in the figure are: a flat background, a double structure at about ± 25 mV and ± 40 mV and a well-defined Pb gap structure at low voltages. Due to the presence of the double structure, there is some ambiguity in extracting the energy gap value from the experiments.

Similar double features are often observed in the tunneling characteristics of Bi-Sr-Ca-Cu-O (Refs. 17–21) as well as in other HTS-based junctions.^{4,22} In earlier indications they have been associated to different phases with different T_c in the junction area²¹ but recent advances in fabricating good quality single phase crystals and films play against this explanation. In some cases, the lower-energy structure has been associated to the Bi-Sr-Ca-Cu-O energy gap and the secondary peak to the HTS phonon modes.^{20–23} However, in conventional junctions, phonon structures are symmetric in voltage, and appear as few percent conductance variations that never exceed the DOS peaks. Other authors¹⁹ consider the possibility that the lower-energy structure is an inner gap as that produced by interlayering pairing in models of layered metallic systems,²⁴ but also in this case no quantitative agreement with theory has been found. Gap anisotropy has also been considered,^{25,26} with reported values close to those found in our measurements. Since no definite conclusion can be drawn from this scenario, we decided to extract the gap value from the most satisfactory fitting of the experimental data.

As is well known, the superconducting structures of the two electrodes are not individually observed in the tunneling characteristics of traditional S - I - S' junctions. However, they are often seen in tunneling experiments in HTS- I - S junctions.^{4,19,27,28} The appearance in Fig. 1 of the Pb superconducting structures can be understood if a finite DOS at the Fermi level of the HTS is supposed. In this case, in fact, at low energies, the high- T_c material behaves as normal and we expect conductance characteristics similar to those of N - I - Pb junctions.

By using a standard procedure,^{3,19,20,29} we have introduced a phenomenological smearing parameter Γ in the BCS expression for the Bi-Sr-Ca-Cu-O DOS:

$$N_S(E, T) = N_N \operatorname{Re} \frac{|E + i\Gamma|}{\sqrt{(E + i\Gamma)^2 - \Delta(T)^2}} \quad (1)$$

The Γ parameter has been firstly introduced by Dynes, Narayanamurti, and Garno³⁰ to describe the effect of lifetime broadening for Cooper pairs. With a suitable choice of the Γ/Δ ratio, a nonzero DOS at the Fermi level is simulated. The use of expression (1) for the density of states of HTS may be justified by stoichiometric variations or by the important role that spin fluctuations play in these materials.

The dotted line in Fig. 1 has been obtained by introducing expression (1) in the conductance expression of a HTS- I -Pb junction at 4.2 K. The values $\Delta=20$ meV, $\Gamma=6$ meV, and $\Delta_{pb}=1.3$ meV have been used in this fitting while no satisfactory agreement has been found when trying to model the secondary structure at higher energies.

We notice that, by using two fitting parameters, the peak voltage position is reproduced quite well by several choices of the Δ and Γ under the condition that $\Delta + \Gamma$ is kept constant. This is observed in Fig. 2 which also indicates that the Γ/Δ ratio is responsible for the amplitude of the HTS structure and for the overall $G(V)$ shape. In the figure, $\Delta + \Gamma = 26$ meV and $\Gamma/\Delta = 0.1, 0.3$, and 0.8 have been supposed. We remark that to obtain a quantitative fitting of the experiments, as in Fig. 1, variations of only a few percent of the Δ and Γ parameters are allowed. In fact, by increasing the Γ/Δ value, in Fig. 2, a progressive reduction and smearing of the Bi-Sr-Ca-Cu-O superconducting structure is observed. At the same time the Pb superconducting features appear more pronounced.

In Fig. 3 we present the I - V and the normalized differential conductance characteristics of a Bi-Sr-Ca-Cu-O/Au junction at $T=4.2$ K. In this case, the I - V curve shows multiple switches and hysteresis that disappear at temperature between 70 and 80 K. These features, due to internal grain boundary junctions, have been often found in Bi-Sr-Ca-Cu-O based junctions.^{18,25,31,32} Such discontinuities in the I - V curves produce peaks in the conductance spectra that can be

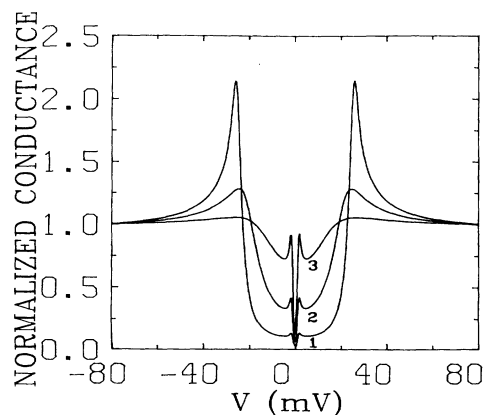


FIG. 2. Normalized conductance characteristics at $T=4.2$ K of an HTS- I -Pb junction obtained from expression (1) with (1) $\Delta=24$ meV, $\Gamma=2$ meV, (2) $\Delta=20$ meV, $\Gamma=6$ meV, and (3) $\Delta=14$ meV, $\Gamma=12$ meV. $\Delta_{pb}=1.3$ meV has been used.

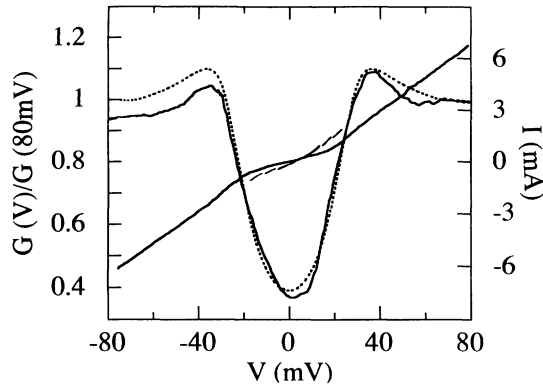


FIG. 3. I - V and normalized conductance characteristics of a Bi-Sr-Ca-Cu-O/Au junction at $T=4.2$ K (full lines). The dotted line is the theoretical fitting obtained from expression (1) with $\Delta=25$ meV, $\Gamma=12$ meV.

easily confused with the HTS gaplike structures.

To avoid this problem, the $G(V)$ vs V curve of Fig. 3 has been numerically computed from the I - V continuous curve. For this junction, a single peak is observed at about ± 30 mV. The dotted line in the figure has been obtained by introducing the modified BCS density of states, expression (1), in the conductance expression for a HTS- I - N junction. The values $\Delta=26$ meV and $\Gamma=12$ meV have been used. The Γ/Δ ratio here is higher than that used to fit the data in Fig. 1. However, the single peak reproduces the envelope of the maxima of Fig. 1 quite well. This fact seems to indicate that, due to a more effective smearing, the double structure is not resolved in the Bi-Sr-Ca-Cu-O/Au junction. More quantitative analysis seems inappropriate at the moment but we remark here that, in our junctions, the appearance of the double structure is not related to the nature of the used counterelectrode.

B. Linear backgrounds

One remarkable feature of the HTS-based tunnel junctions is the linear dependence of the background conductances with voltages until few hundreds of meV. This peculiarity is routinely found in junctions fabricated on Y-Ba-Cu-O (Refs. 4, 5, and 27), La-Sr-Cu-O (Ref. 11), and Tl-Ba-Ca-Cu-O (Ref. 31) as well as on the bismuth oxides Ba-Pb-Bi-O (Ref. 33) and Ba-K-Bi-O (Refs. 33 and 34). We have found it in about 40% of the Bi-Sr-Ca-Cu-O measured junctions.

In Fig. 4(a), as an example, the $G(V)$ vs V of a Bi-Sr-Ca-Cu-O/Pb-Bi junction is reported at 4.2 K. The Bi-Sr-Ca-Cu-O double structure appears more smeared than in the data shown in Fig. 1 with a broad relative maximum around ± 25 mV.

In Fig. 4(b), for comparison, the $G(V)$ vs V characteristic of a Y-Ba-Cu-O/Pb junction with $T_c=87$ K is reported at 4.2 K. The same fabrication technique has been used for this junction. A striking similarity in the overall shape of the experimental data is observed in Figs. 4(a) and (b) with the Y-Ba-Cu-O junction presenting a

gaplike structure at about ± 25 mV and a second structure at about ± 40 mV.

In effect, the double structure appears much more evident in fully oxygenated Y-Ba-Cu-O junctions,⁵ and we have observed that, for this material, the structure amplitude is reduced by inducing oxygen deficiency at the surface.³⁵ It seems plausible to extend these considerations also to the Bi-Sr-Ca-Cu-O junctions and speculate that, in comparison with Fig. 1, in Figs. 3 and 4(a) some nonstoichiometric oxygens at the surface could be responsible for the reduction of the secondary structure.

In the insets of Figs. 4(a) and 4(b), the low-bias I - V characteristics are shown for the same junctions. The full lines in the insets are the theoretical fittings obtained from the expression for the current flowing through a N - I - S junction at 4.2 K. In these calculations the HTS have been considered as normal since both show finite conductance in the studied energy range. The values $\Delta_{\text{Pb-Bi}}=1.6$ meV and $\Delta_{\text{Pb}}=1.3$ meV for the Pb-Bi and Pb

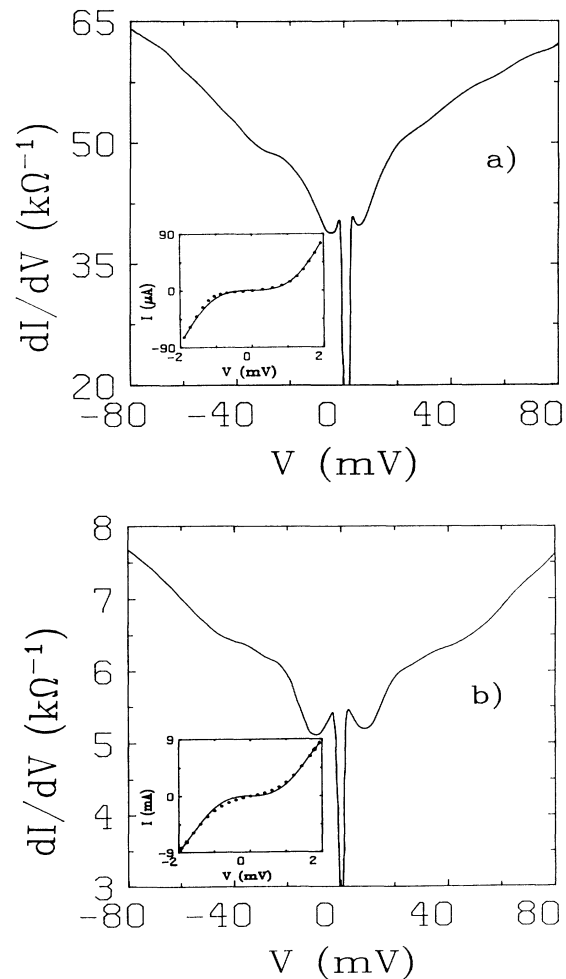


FIG. 4. Conductance characteristics vs voltage, at $T=4.2$ K, of a Bi-Sr-Ca-Cu-O/Pb-Bi (curve a), and an Y-Ba-Cu-O/Pb junction (curve b). Insets: low-bias I - V characteristics for the same junctions; the full lines are the theoretical fittings for the current flowing through an S - I - N junction at the same temperature.

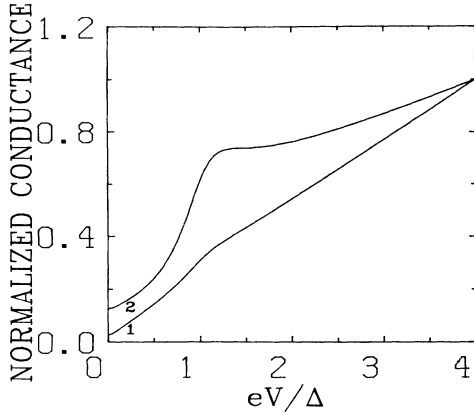


FIG. 5. Normalized conductance characteristics of HTS- I - N junctions with different linear backgrounds. Expression (2) has been used with $\Delta=20$ meV, $\Gamma=6$ meV and (1) $\alpha=7\times 10^{-2}$ meV $^{-1}$, $\sigma=0.4$ and (2) $\alpha=7\times 10^{-3}$ meV $^{-1}$, $\sigma=0.4$.

counterelectrodes have been used. The satisfactory agreement between experiments and theory indicates negligible leakage currents and the barriers are so proven to be continuous and pin hole free in both junctions.³⁶ This fact seems to indicate that, at least at low energies, the mechanism responsible for the linear background is not due to spurious effects in the tunnel barrier.

In the case of a linear background we have studied the effect that this has on the superconducting structures of the high- T_c material. In a recent paper³⁷ the HTS density of states has been expressed by adding a BCS-like contribution to a linear one. Consequently, the conductance characteristics of a HTS- I - N junction can be written as

$$G(V, T) = \sigma \int_{-\infty}^{+\infty} \text{Re} \left[\frac{(E + i\Gamma)^2}{(E + i\Gamma)^2 - \Delta(T)^2} \right]^{1/2} \frac{\partial f(E + eV)}{\partial V} dE \\ + \alpha \int_{-\infty}^{+\infty} |E| \frac{\partial f(E + eV)}{\partial V} dE \quad (2)$$

with σ and α representing the conductance intercept at $V=0$ and the conductance slope as inferred from the high-bias data at low temperatures.

The curves in Fig. 5 have been obtained from expression (2) with $\Delta=20$ meV and $\Gamma=6$ meV while the coefficient of the linear term α has been changed by one order of magnitude. It is so clear that a progressive reduction of the superconducting structure of the HTS is produced and only a change of slope is observed for steeper backgrounds.

C. Zero-bias anomalies

Let us consider now another kind of anomalous behavior that we have found in the tunneling characteristics of about 30% of the measured junctions independently from the presence of constant or linear backgrounds. In fact, a conductance peak centered at zero bias is often observed in the tunneling spectra of high- T_c materials.^{3,6,38-40} Recently, detailed reports on this topic have appeared in the literature.⁴¹⁻⁴³ Even if the anomaly develops around $V=0$, in some cases its amplitude reaches several tens of mV. We have included it in the present background analysis since interference with the super-

conducting structures of both electrodes can take place.

The study of the anomaly behavior has been the object of another paper⁴³ and it has been found that, in the case of logarithmic dependence on both energy and temperature, the excess conductance peak is due to a Kondo-type scattering that accounts for electron magnetic interactions at the barrier interface.⁴⁴⁻⁴⁷ Here we want to focus on the influence that, depending on their voltage amplitude, these anomalies have on the superconducting structures of both the high- T_c material and the Pb counterelectrode.

In Fig. 6(a) we have plotted the low-bias conductance data of a BSCCO/Pb junction, at 4.2 K. The curve reveals narrow maxima at about ± 2 mV together with some oscillations at higher biases. Even though they appear anomalous, these features seem to be related to the Pb gap and phonon structures, present at the same temperature.

In these cases more insight can be achieved from the analysis of the conductance temperature behavior. As shown in Fig. 6(b), at $T=10$ K, with the Pb in the normal state, a conductance peak centered at zero bias is present in the $G(V)$ vs V curve for the same junction. The anomaly is about 10% of the background conductance (dotted line) with a voltage amplitude of about ± 6 mV. We have found that the peak appears at about 50 K and, for $T > T_{cPb}=7.2$ K, logarithmically increases for decreasing temperatures.⁴³ For temperatures below 7.2 K, the Pb superconducting structures start to merge, and at $T=4.2$ K, these completely mask the zero-bias anomaly.

In conventional junctions the anomaly develops above the junction T_c and its temperature and voltage behavior at low temperatures is studied in (low) magnetic fields with both electrodes in the normal state.^{44,45} The measured N - I - N' conductance is written as

$$G(V, T) = G_0(V, T) + \Delta G(V, T), \quad (3)$$

where $G_0(V, T)$ is the background conductance and $\Delta G(V, T)$ is the excess conductance defined as the difference between the total and background conductance:⁴⁵⁻⁴⁷

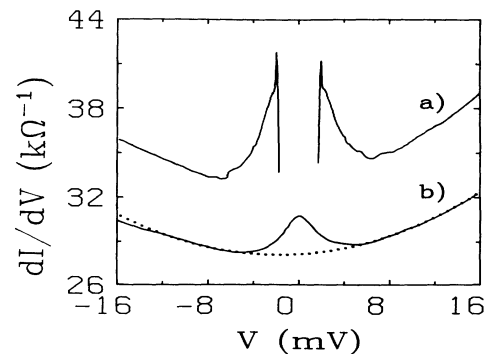


FIG. 6. Conductance characteristics vs voltage at low bias for a Bi-Sr-Ca-Cu-O/Pb junction, at $T=4.2$ K (curve a) and at $T=10$ K (curve b). The dotted line shows the extrapolated parabolic background.

$$\Delta G(V, T) \propto N_L N_R \ln \left[\frac{E_0}{(e|V| + nk_B T)} \right], \quad (4)$$

where N_L and N_R are the normal DOS of the left and right electrodes, E_0 is a cutoff energy, n is a numerical factor close to unity, and k_B is the Boltzman constant.

Let us suppose that, in an HTS-I-Pb junction, Cu isolated moments are responsible for the conductance peak at zero bias. At low voltages and for $T \approx 0$ K, as a first approximation, both G_0 and ΔG include the conventional electrode superconducting DOS so that the normalized conductance can be written as

$$\tilde{G}(V) = \text{Re} \left[\frac{|eV + i\Delta'|}{\sqrt{(eV + i\Delta')^2 - \Delta^2}} \right] \times \left[A \ln \frac{E_0}{(e|V| + nk_B T)} + 1 \right], \quad (5)$$

where A takes into account the intensity of the zero-bias anomaly (ZBA) and, by an usual procedure, the Δ' parameter has been introduced to eliminate the divergence of the Pb density of state at $T = 0$ K.

In Fig. 7 the full lines represent the two bracketed terms in expression (5), i.e., the Pb density of state with $\Delta = 1.3$ meV and $\Delta' = 0.1$ meV and a 20% ZBA with a cutoff energy $E_0 = 10$ meV. The dotted line in the figure is the full expression (5) that reproduces the main experimental features observed in Fig. 6(a) at $T = 4.2$ K. In fact, the voltage at which the Pb gap structures appear is not greatly affected by the presence of the ZBA; however, these features have a higher intensity and a wider voltage amplitude. We remark that, by this first approximation analysis, due to the ZBA voltage amplitude (reflected in the cutoff energy $E_0 = 10$ meV) the Bi-Sr-Ca-Cu-O superconducting structures at higher energy are not affected. In fact, we have experimentally observed the HTS gaplike structures at about ± 25 meV in the junction of Fig. 6(a).

We have found a completely anomalous behavior in the case of another Bi-Sr-Ca-Cu-O/Pb junction whose tunneling characteristics at different temperatures are reported in Fig. 8. At $T = 20$ K, a conductance maximum

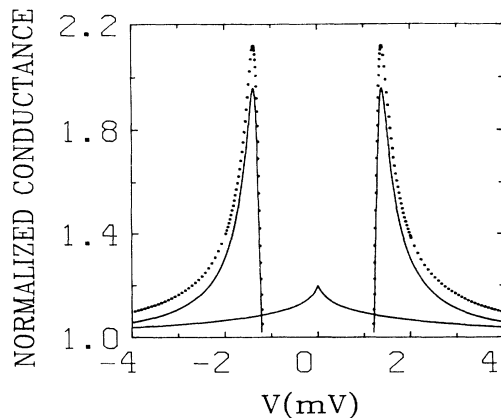


FIG. 7. Full lines: the Pb density of state and a 20% ZBA. Dotted line: normalized conductance characteristic at $T \approx 0$ K obtained from expression (5).

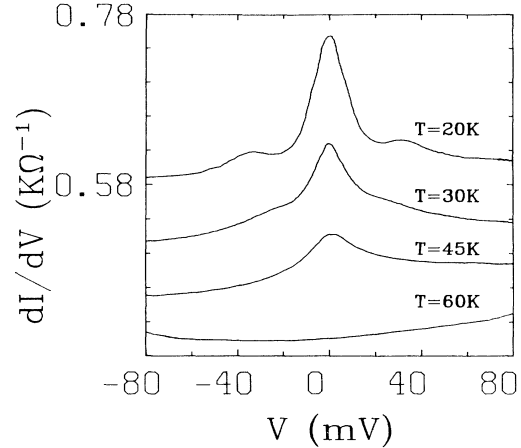


FIG. 8. Conductance characteristics vs voltage, at different temperatures, of a Bi-Sr-Ca-Cu-O/Pb tunnel junction; the vertical axis has been shifted for clarity.

at zero bias is observed together with a pronounced structure that develops between ± 20 mV and ± 40 mV and a decreasing background at high biases. Once again, the temperature behavior reveals that a zero-bias anomaly appears at about 55 K. The anomaly is superimposed to a highly asymmetric background that, for higher temperatures, shows the traditional parabolic behavior.^{48,49} This giant conductance peak shows a logarithmic dependence on energy and temperature with an intensity of $\approx 50\%$ with respect to the background and a voltage amplitude of about ± 50 mV at low temperatures. In this voltage range, interference of the anomaly with the Bi-Sr-Ca-Cu-O superconducting structures is to be expected. In the past, similar extremely anomalous behaviors have been found in semiconductor-metal junctions.^{50,51}

Let us assume that both semiconducting regions, responsible for the Kondo effect, and superconducting regions are present at the Bi-Sr-Ca-Cu-O surface. In this case, by keeping the conventional counterelectrode in the normal state, as a first approximation, at $T \approx 0$ K, expression (3) can be written as

$$\tilde{G}(V) = (1 - \beta) \text{Re} \left[\frac{|eV + i\Gamma|}{\sqrt{(eV + i\Gamma)^2 - \Delta^2}} \right] + \beta \left[A \ln \frac{E_0}{(e|V| + nk_B T)} + 1 \right], \quad (6)$$

where β takes into account the percentage of semiconducting regions in the junction area.

In Fig. 9 the full lines represent the bracketed terms in expression (6), i.e., the Bi-Sr-Ca-Cu-O density of states with $\Delta = 20$ meV and $\Gamma = 10$ meV and a 50% ZBA with a cutoff energy $E_0 = 60$ meV, respectively. The dotted line in the figure represents the full expression (6) in which 80% semiconducting regions have been supposed. One can observe that it satisfactorily reproduces the main experimental behavior at lower temperatures, that is, the inversion of the overall conductance shape, that, even in case of 20% superconducting regions, still shows the signature of the Bi-Sr-Ca-Cu-O superconducting structures. These are shifted in energy and superimposed to a slightly decreasing background.

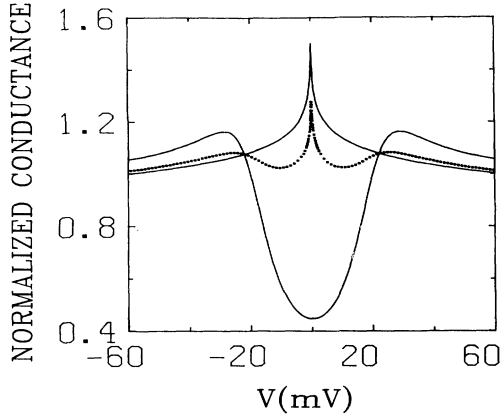


FIG. 9. Full lines: the Bi-Sr-Ca-Cu-O density of state with $\Delta = 20$ meV and a 50% ZBA. Dotted line: conductance characteristic at $T \approx 0$ K obtained from expression (5). An 80% percentage of semiconducting surface regions has been supposed.

III. CONCLUSIONS

We have analyzed the different conductance backgrounds of tunneling spectra of the 2-2-1-2 Bi-Sr-Ca-Cu-O system. In the case of traditional constant behavior at high biases, we have focused on the superconducting double structure which is very similar to that observed for the 1-2-3 Y-Ba-Cu-O system. We think that the origin of this feature is an important key for the understanding of the mechanism responsible for the superconductivity in the HTS and that the wide spreading of the Bi-Sr-Ca-Cu-O energy gap values reported in the literature is mainly due to the fact that, in the experiments, the structure is not always well resolved.

Excluding cases with a high degree of smearing ($\Gamma > 0.3\Delta$), the whole set of experimental data has been fitted by a modified BCS DOS from which an average $\Delta = 20 \text{ meV} \pm 2 \text{ meV}$, corresponding to $2\Delta/k_B T_c = 5.8$, is inferred. These values are close to those found in experiments carried out on Y-Ba-Cu-O based tunnel junctions.^{4,5} Since the role of the CuO_2 superconducting planes is of primary importance in the cuprate oxides, we conjecture that the main structure at about 20 meV is confined in these planes in both the Y-Ba-Cu-O and Bi-Sr-Ca-Cu-O systems. Flat backgrounds may be also related to the CuO_2 superconducting layers. Their more frequent observation in the Bi-Sr-Ca-Cu-O compound with respect to other HTS can be reconciled with the fact

that the CuO_2 planes are spatially well separated with weak interplane coupling in this material.^{9,52}

As we have already mentioned, in order to reproduce the experimental conductances, a phenomenological Γ parameter has been introduced in the BCS expression for the DOS of the high- T_c material. The analysis of the tunneling characteristics of HTS-I-S junctions has then revealed that the counterelectrode superconducting structures are evidenced for increasing values of the Γ/Δ ratio. At the moment, it seems quite arbitrary to place too much significance on the physical origin of this smearing factor, since sample inhomogeneities, such as oxygen not perfect stoichiometry, may still be limiting the reproducibility of the experimental results.

Linear conductance backgrounds are perhaps the most fundamental empirical difference between the high- T_c materials and traditional superconductors. The origin of this linear term is matter of an intense debate. Our experiments are not able to give more insight about this topic; however, we clearly show that for increasing slopes of the background conductance, the superconducting features of the HTS are progressively smeared and reduced in amplitude. This fact adds more indetermination in inferring the energy gap values from the experiments.

We remark that, if the linear term is intrinsic, it may still have substantial variations from one material to another. In this respect, specific heat measurements also indicate that the linear term is not present in the Bi-Sr-Ca-Cu-O compound or is at least one order of magnitude smaller than that observed for the 1-2-3 Y-Ba-Cu-O system.⁵³

Finally, we have studied the effects that a zero-bias conductance peak has on the tunneling characteristics of the HTS. The behavior of these anomalies is explained in terms of electron magnetic interactions at the tunnel barrier. Depending on their voltage amplitude, isolated Cu moments at the interface or, in case of highly asymmetric backgrounds, semiconducting surface regions can be supposed. From a closer analysis of the conductance curves, clear interferences with the superconducting structures of both the conventional counterelectrode and the high- T_c material are observed.

In conclusion, we think that anomalous backgrounds contribute to the uncertainty in the determination of the high- T_c superconducting parameters and a great care has to be taken for a better diagnostics on the tunneling spectra of these materials.

¹For a recent review, see T. Hasegawa, H. Ikuta, and K. Kitazawa, in *Physical Properties of High- T_c Superconductors III*, edited by D. M. Ginsberg (World Scientific, Singapore, 1992).

²H. Ikuta, A. Maeda, K. Uchinokura, and S. Tanaka, *Jpn. J. Appl. Phys.* **27**, L1038 (1988).

³T. Ekino and J. Akimitsu, *Phys. Rev. B* **40**, 6902 (1989).

⁴M. Gurvitch, J. M. Valles, Jr., A. M. Cucolo, R. C. Dynes, J. P. Garno, L. F. Schneemeyer, and J. V. Waszczak, *Phys. Rev. Lett.* **63**, 1008 (1989); *Phys. Rev. B* **44**, 11 986 (1991).

⁵A. M. Cucolo, R. C. Dynes, J. M. Valles, Jr., and L. F. Schneemeyer, *Physica C* **179**, 69 (1991).

⁶Q. Huang, J. F. Zasadzinski, K. E. Gray, J. Z. Liu, and H.

Claus, *Phys. Rev. B* **40**, 93 666 (1989).

⁷R. Escudero, E. Guarner, and F. Morales, *Physica C* **166**, 15 (1990).

⁸M. Suzuki, H. Inone, and L. Rinderer, *Phys. Rev. B* **41**, 7217 (1990).

⁹T. Hasegawa and K. Kitazawa, *Jpn. J. Appl. Phys.* **29**, L434 (1990).

¹⁰A. M. Cucolo, R. Di Leo, and A. Nigro, *Physica C* **207**, 21 (1993).

¹¹J. R. Kirtley and D. J. Scalapino, *Phys. Rev. Lett.* **65**, 798 (1990).

¹²P. W. Anderson and Z. Zou, *Phys. Rev. Lett.* **60**, 132 (1988).

- ¹³C. W. Varma, P. B. Littlewood, S. Schnitt-Rink, E. Abrahams, and A. E. Ruckenstein, *Phys. Rev. Lett.* **63**, 1996 (1989).
- ¹⁴J. C. Phillips, *Phys. Rev. Lett.* **59**, 1856 (1987).
- ¹⁵A. M. Cucolo, J. M. Valles, R. C. Dynes, M. Gurvitch, J. M. Phillips, and J. P. Garno, *Physica C* **161**, 351 (1989).
- ¹⁶R. P. Vasquez and R. M. Housley, *J. Appl. Phys.* **67**, 7141 (1990).
- ¹⁷J. Liu, J. Wan, A. M. Goldman, Y. C. Chang, and P. Z. Jiang, *Phys. Rev. Lett.* **67**, 2195 (1991).
- ¹⁸A. M. Cucolo, R. Di Leo, P. Romano, and G. Balestrino, *Physica C* **180**, 208 (1991).
- ¹⁹H. J. Tao, A. Clang, Farun Lu, and E. L. Wolf, *Phys. Rev. B* **45**, 10 622 (1992).
- ²⁰S. I. Vedeneev, P. Samuely, S. V. Meshkov, G. M. Eliashberg, A. G. M. Jansen, and P. Wyder, *Physica C* **198**, 47 (1992).
- ²¹Kussumaul, J. S. Moodera, G. M. Roesler, and P. M. Tedrow, *Phys. Rev. B* **41**, 842 (1990).
- ²²A. P. Fein, J. R. Kirtley, and M. W. Shafer, *Phys. Rev. B* **37**, 9738 (1988).
- ²³N. A. Tulina, S. V. Zaitsev, G. A. Emel'chenko, M. P. Kulakov, N. N. Kalesnikov, and N. S. Sidorov, *Physica C* **194**, 370 (1992).
- ²⁴R. A. Klemm and S. H. Liu, *Phys. Rev. B* **44**, 7526 (1991); **45**, 415 (1992).
- ²⁵M. Boekholt, M. Hoffmann, and G. Guntheroldt, *Physica C* **175**, 127 (1991).
- ²⁶L. Buschmann, M. Boekholt, and G. Guntheroldt, *Physica C* **203**, 68 (1992).
- ²⁷M. Lee, M. Naito, A. Kapitulnik, and M. R. Beasley, *Solid State Commun.* **70**, 449 (1989).
- ²⁸S. I. Vedeneev, P. Samuely, A. G. M. Jansen, I. P. Kazakov, and R. Gonnelli, *Z. Phys. B* **83**, 343 (1991).
- ²⁹Z. Zhang and C. M. Lieber, *Phys. Rev. B* **47**, 3423 (1993).
- ³⁰R. C. Dynes, V. Narayanamurti, and J. P. Garno, *Phys. Rev. Lett.* **41**, 1509 (1978).
- ³¹I. Takeuchi, J. S. Tsai, Y. Shimakawa, T. Manako, and Y. Kubo, *Physica C* **158**, 83 (1989).
- ³²T. Walsh, J. Moreland, R. H. Ono, and T. S. Kalkur, *Phys. Rev. B* **43**, 11 492 (1991).
- ³³F. Sharifi, A. Pargellis, R. C. Dynes, B. Miller, E. S. Hellman, J. Rosamilia, and E. H. Hartford, Jr., *Phys. Rev. B* **44**, 12 521 (1991).
- ³⁴J. F. Zasadzinski, N. Tralshawala, Q. Huang, K. E. Gray, and D. G. Hinks, *IEEE Trans. Magn.* **MAG-27**, 833 (1991).
- ³⁵A. M. Cucolo, R. Di Leo, P. Romano, L. F. Schneemeyer, and J. V. Waszczak, *Phys. Rev. B* **44**, 2857 (1991).
- ³⁶A. M. Cucolo, *Int. J. Mod. Phys. B* **7**, 2549 (1993).
- ³⁷A. M. Cucolo, C. Noce, and A. Romano, *Phys. Rev. B* **46**, 5864 (1992); *Physica C* **202**, 33 (1993).
- ³⁸M. Lee, D. B. Mitzi, A. Kapitulnik, and M. R. Beasley, *Phys. Rev. B* **39**, 801 (1989).
- ³⁹J. S. Tsai, I. Takeuchi, J. Fujita, S. Miura, T. Terashima, Y. Bando, K. Iijima, and K. Kamamoto, *Physica C* **157**, 537 (1989).
- ⁴⁰D. Mandrus, L. Forro, D. Koller, and L. Mihaly, *Nature* **351**, 460 (1991).
- ⁴¹T. Walsh, J. Moreland, R. H. Ono, and T. S. Kalkur, *Phys. Rev. Lett.* **66**, 516 (1991).
- ⁴²J. Lesueur, L. H. Greene, W. L. Feldmann, and A. Inam, *Physica C* **191**, 326 (1992).
- ⁴³A. M. Cucolo and R. Di Leo, *Phys. Rev. B* **47**, 2916 (1993).
- ⁴⁴A. F. G. Wyatt, *Phys. Rev. Lett.* **13**, 401 (1964).
- ⁴⁵L. Y. L. Shen and J. M. Rowell, *Phys. Rev.* **165**, 566 (1968).
- ⁴⁶J. A. Appelbaum, *Phys. Rev. Lett.* **17**, 91 (1966); *Phys. Rev.* **154**, 633 (1967).
- ⁴⁷P. W. Anderson, *Phys. Rev. Lett.* **17**, 95 (1966).
- ⁴⁸J. G. Simmons, *J. Appl. Phys.* **34**, 1793 (1963).
- ⁴⁹W. F. Brinkman, R. C. Dynes, and J. M. Rowell, *J. Appl. Phys.* **41**, 1915 (1970).
- ⁵⁰E. L. Wolf and D. L. Loose, *Phys. Rev. B* **2**, 3660 (1970).
- ⁵¹R. A. Logan and J. M. Rowell, *Phys. Rev. Lett.* **13**, 404 (1964).
- ⁵²T. Hasegawa, M. Nantoh, H. Ikuta, and K. Kitazawa, *Physica C* **185**, 1743 (1991).
- ⁵³R. A. Fisher, S. Kim, S. E. Lacy, N. E. Phillips, D. E. Morris, A. G. Markelz, J. Y. T. Wei, and D. S. Ginley, *Phys. Rev. B* **38**, 11 942 (1988).